Counter-rotating type axial flow pump unit in turbine mode for micro grid system

Counter-rotating type axial flow pump unit in turbine mode for micro grid system

R Kasahara[1], G Takano[1], T Murakami[2], T Kanemoto[2] and K Komaki[1]

[1] Graduate School of Engineering, Kyushu Institute of Technology, Kitakyushu, Fukuoka, Japan
[2] Faculty of Engineering, Kyushu Institute of Technology, Kitakyushu, Fukuoka, Japan

E-mail: h104034r@tobata.isc.kyutech.ac.jp

Abstract. Traditional type pumped storage system contributes to adjust the electric power unbalance between day and night, in general. This serial research proposes the hybrid power system combined the wind power unit with the pump-turbine unit, to provide the constant output for the grid system, even at the suddenly fluctuating/turbulent wind. In the pumping mode, the pump should operate unsteadily at not only the normal but also the partial discharge. The operation may be unstable in the rising portion of the head characteristics at the lower discharge, and/or bring the cavitation at the low suction head. To simultaneously overcome both-weak points, the authors have proposed a superior pump unit that is composed of counter-rotating type impellers and a peculiar motor with double rotational armatures. This paper discusses the operation at the turbine mode of the above unit. It is concluded with the numerical simulations that this type unit can be also operated acceptably at the turbine mode, because the unit works so as to coincide the angular momentum change through the front runners/impellers with that thorough the rear runners/impellers, namely to take the axial flow at not only the inlet but also the outlet without the guide vanes.

1. Introduction

To cope with the warming global environment and the energy crisis, the hydropower should occupy the attention of the electric power generation as clean and cool energy resources with the highest density, in cooperation with wind and solar powers. That is, we should make effort to utilize effectively not only the large but also the small/mini/micro hydropower at the onshore and the offshore without nature disruptions.

The authors have invented the unique pumping unit in order to suppress the unstable performance and the cavitation [1, 2]. In the unit, a new type of the AC induction motor with the double rotational armatures in place of the traditional mechanism has been developed. The inner and the outer armatures drive the front and the rear impellers, respectively, while the relative rotational speed between both armatures is kept constant and that the rotational torque is counter-balanced between both impellers/armatures. Then, the angular momentum change through the front impeller must be the same as that through the rear impeller. Such operating conditions play important parts in adjusting automatically the front and the rear impeller works in response to the discharge, and then suppress successfully the unstable operation at the low discharge and the cavitation at the high discharge. The authors have called such features ‘‘smart control’’ for twelve years [1]. Furthermore, the authors have also invented the counter-rotating type hydroelectric unit, which is composed of the tandem runners

and the peculiar generator with double rotational armatures [3]. The unit has fruitful advantages that not only the induced voltage is sufficiently high without supplementary equipment such as a gearbox, but also the rotational moment hardly acts on the mounting bed because rotational torque counter-balances in armatures/runners. The performances and the flow conditions of the runners have been investigated [4] and design materials for runners have been also presented [5]. The tandem runners have also proposed by Prof. Nielsen [6]

The objective of the serial researches is to confirm that the counter-rotating type can be provided for not only the pumping mode but also the turbine mode. This paper discusses the turbine mode of the counter-rotating type axial flow pump, as the preliminary step.

2. Experimental and numerical simulation

2.1. Experimental setup

Figure 1 shows the model pumping unit with the AC induction motor. The inner and the outer armatures in the motor are connected directly to the front and the rear impellers, respectively. The major specifications at the design point are the theoretical head H = 4.4 m, the discharge Q = 1.78 m^3/min, and the individual impeller speed $n_F = n_R$ = 1500 min^{-1} (subscripts F and R denote the front and the rear impellers). The specific speed of the individual impeller is N_S = 1100 m, m^3/min, min^{-1}, and the specific speed as the pumping unit with the counter-rotating type impellers is N_{ST} = 1320 m, m^3/min, min^{-1}. The impeller diameters are 150 mm, and the boss ratio is 0.4. The numbers of the front and rear blades are 5 and 4, respectively. The blade profiles are shown in figure 2 and the dimensions are given in table 1, where $R\Theta$ and Z are the distances in the circumferential/tangential and the axial directions divided by the impeller diameter, β_d is the inlet and the outlet angles of the blades measured from the axial direction (subscripts 1 to 4 denote the inlet and outlet of the front and rear impellers, respectively). Impeller A was designed with the traditional procedure as follows. The blade thickness derived from NACA4409 hydrofoil [7] was distributed on the camber line of the single arc, and the twist center was placed on the center of the camber line. The solidities of the front and rear cascades are 0.75 regardless of the radial position. On the contrary, Impeller B was designed with the 3-D inverse method to improve the pump performance more and more [8]. The solidities of Impeller B are larger than those of Impeller A to suppress the flow separation and slip at the outlet. The blade thicknesses are 0.8 times as thick as those of Impeller A in consideration of the material strength and the decrease of the hydraulic losses.

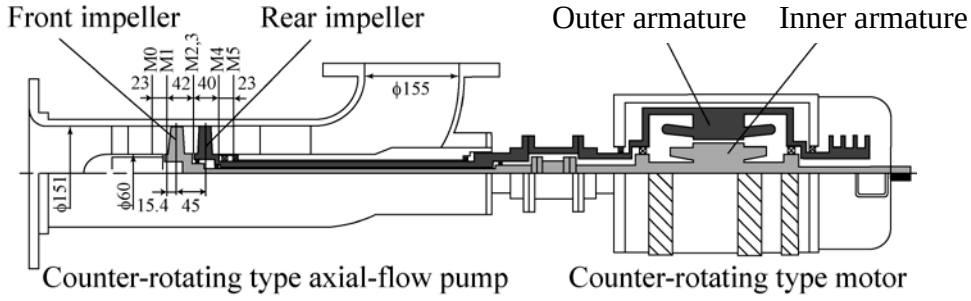

Figure 1. Model counter-rotating type pumping unit

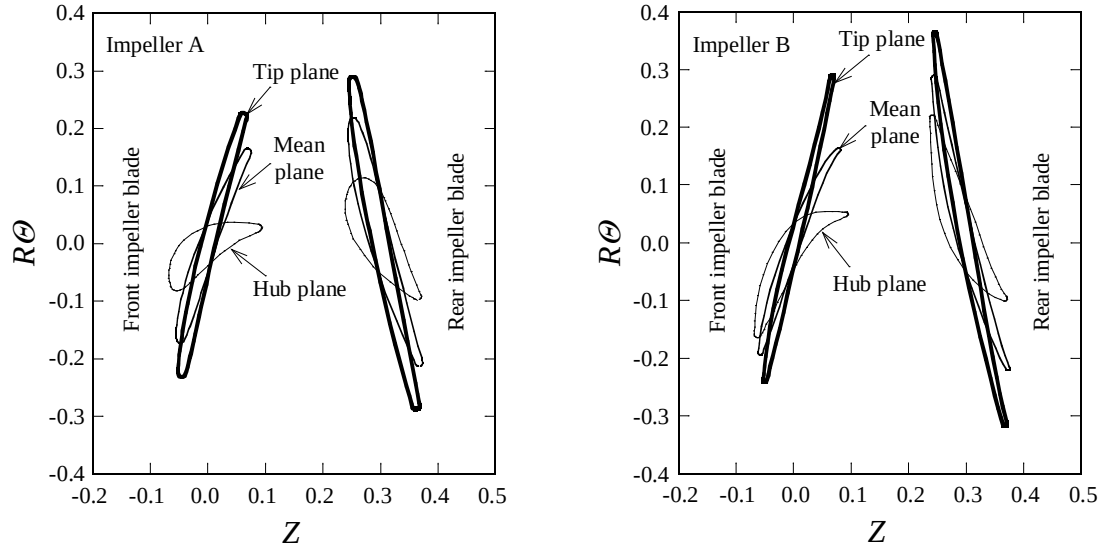

Figure 2. Blade profiles of the counter-rotating type impellers

2.2. Numerical simulation Method

The 3-D turbulent flow in the impeller was simulated at the steady state condition, with the commercial CFD code of ANSYS-CFX ver.12 with SST turbulent model. Figure 3 shows the domains having one of the front impeller/runner passages and one of the rear impeller/runner passages, where the both domains were separated at the section M2, 3 in figure 1. The number of the grid is about 400,000 in the front rotating domain and about 470,000 in the rear rotating domain. Although the pitch-wise length of the front rotating domain differs from that of the rear rotating domain owing to the difference of the blade number, there is no adverse effects in simulation because the circumferentially averaged value was transferred at the boundary between both domains. Then, the circumferential flow distortion at upstream domain is not affects the downstream domain but the distortion in the radial direction domain is taken into consideration in the simulation. Besides, the pitch-wise next-domain neighbour was connected by the periodic boundary.

Table 1. Blade angles and solidities

	Hub_A	$Mean_A$	Tip_A	Hub_B	$Mean_B$	Tip_B
β_{d1}	-67.0	-77.4	-80.4	-76.9	-79.2	-80.4
β_{d2}	0.0	-63.0	-72.6	-14.9	-58.0	-79.0
β_{d3}	77.9	80.0	81.6	71.9	77.2	79.9
β_{d4}	57.7	69.4	76.4	42.9	70.1	75.9
Front(Solidity)	0.75	0.75	0.75	0.99	0.82	0.81
Rear(Solidity)	0.75	0.75	0.75	0.89	0.82	0.78

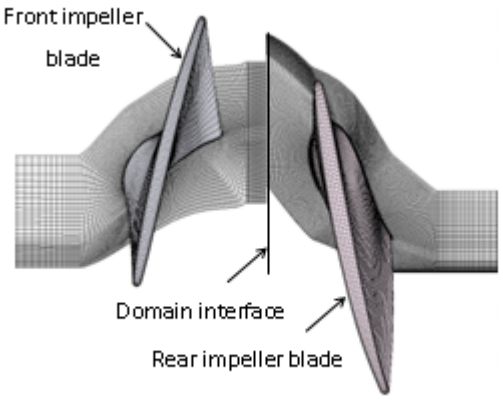

Figure 3. Computational domains and mesh (Impeller A)

3. Validity of the numerical simulation

In order to verify the validity of the numerical simulation, the pump efficiencies were compared with the experimental results in figure 4. In the experiment and the simulation, the relative rotational speed between the front and the rear impellers was kept constant at n_T = 3000 min^{-1}. In this figure, Q/Q_D is the discharge ratio (subscript D: design point), η is the pump efficiency (=$\rho gQH/P$, H is the pump head estimated from the static pressure measured at the casing walls of section M0 and M5 in figure 1, and P is the input power to the motor). The numerically predicted pump efficiencies agree well with the experimental ones in both impellers.

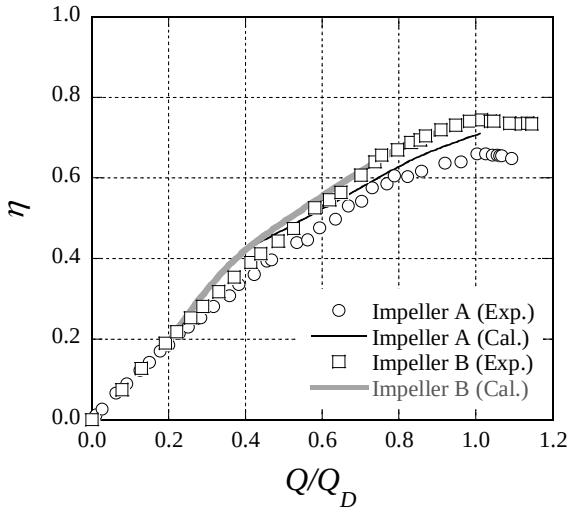

Figure 4. Comparison between experiment and numerical simulation on pump efficiencies

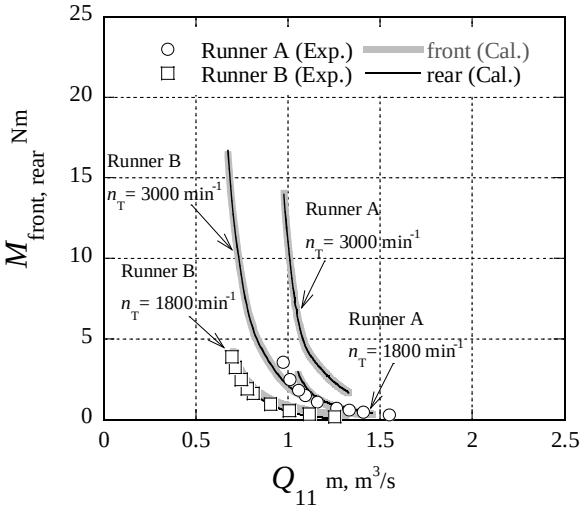

Figure 5. Rotational torques of the front and the rear runners (numerical simulation)

4. Performances in turbine mode

While changing the through flow and the rotational directions of the above impellers without any dimensional modifications, the performances were predicted with the help of numerical flow analysis in the turbine mode. The relative rotational speed between the front runner and the rear runner was kept constant n_T = 3000 min^{-1} while counter-balancing the rotational torque in the same as the pumping mode, where the front and the rear runners in the turbine mode corresponding to the rear and the front impellers in the pumping mode. The relative rotational speed n_T = 3000 min^{-1} corresponds to 50 Hz induced from the double rotational armature type generator with 2 poles, and n_T = 1800 min^{-1}

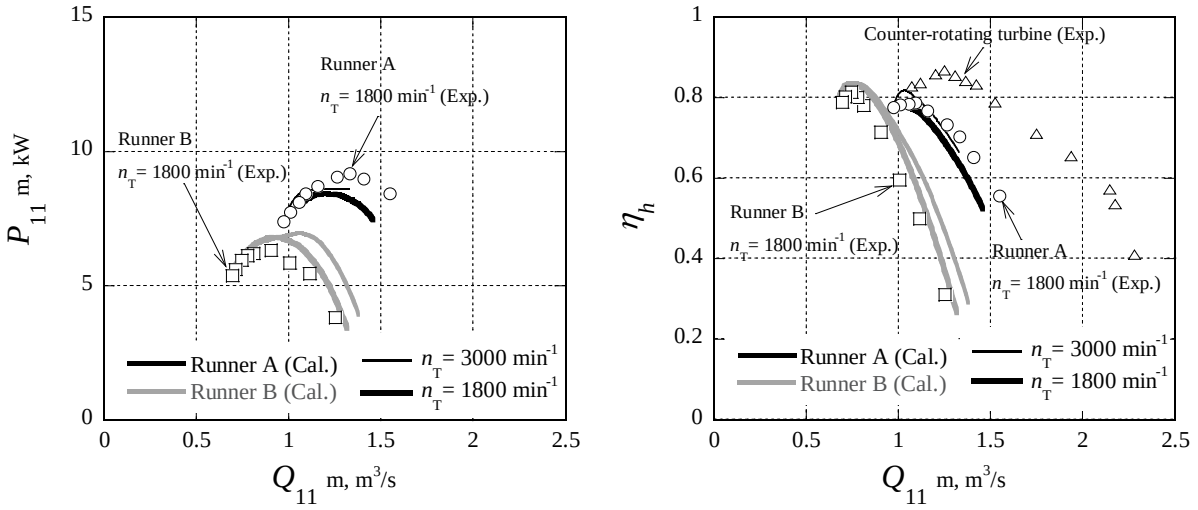

(a) Unit output (b) Hydraulic efficiency

Figure 6. Turbine performances

corresponding to 60 Hz induced from the generator with 4 poles. Figure 5 proves that the rotational torques are counter-balanced between both runners, where Q_{11} is the unit discharge (= $Q/D^2/H^{1/2}$: m, m^3/s), M is the shaft torque, and the solid marks are the experimental results (Exp.), Runner A and Runner B are the runner profiles in the turbine mode of Impeller A and Impeller B given in figures 2 and 4.

Figure 6 shows the turbine performances, where P_{11} is the unit output (=$P/D^2/H^{3/2}$: m, kW) and η_h is the hydraulic efficiency [=$P/(\rho gQH)$]. Runner A takes the maximum output at the higher discharge than that of Runner B as shown in figure 6(a), which is added up with the flow conditions discussed latter. That is, Runner A is suitable for the higher discharge and the lower head, namely has the high specific speed. In figure 6(b), the triangle solid marks denote the experimental result of the counter-rotating type hydroelectric unit designed exclusively for the turbine mode [9]. The maximum hydraulic efficiencies of Runner A and Runner B come close to the efficiency of the above hydroelectric unit regardless of the relative rotational speed, even though Runners A and B are designed exclusive for the pumping mode.

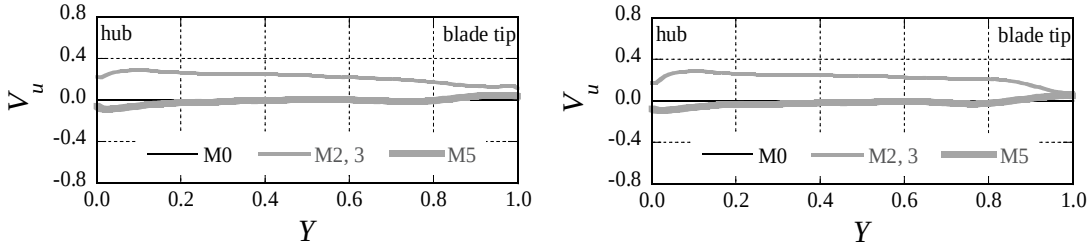

n_T = 3000 min^{-1}, Q_{11} = n_T = 1800 min^{-1}. O_{11} =

(a) Runner A

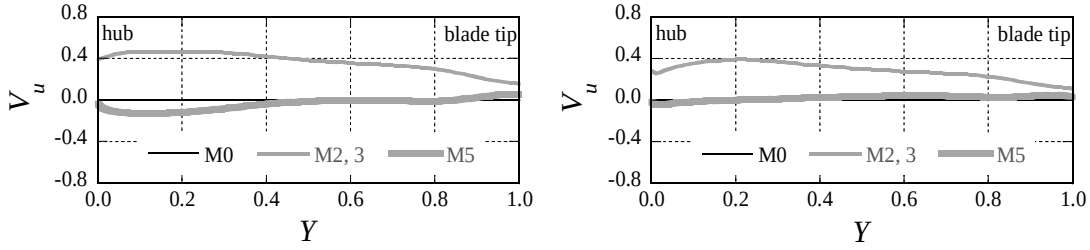

n_T = 3000 min^{-1}, Q_{11} = n_T = 1800 min^{-1}, Q_{11} =

(b) Runner B

Figure 7. Predicted velocity distributions in the radial direction

5. Flow conditions in turbine mode

Figure 7 shows the velocity distributions in the radial direction around the runners at the discharge giving the maximum hydraulic efficiency, where Y is the dimensionless distance from the hub to the casing walls, V_u is the swirling velocity component divided by the relative speed of the blade tip. The axial flow at not only the front runner inlet M0 but also the rear runner outlet M5 hardly have the swirling velocity component, as expected and confirmed in the previous researches [10, 11] regardless of the pumping/turbine mode and/or the blade profiles.

Figure 8 shows the angle of attack at the root-mean-square radius, where the angle was predicted with the average flow angle at 5 mm upstream and 5 mm downstream sections of the runner. The angles against Q_{11} have the similar distributions for the front or the rear blade irrespective of the runner profile, though the values differ each other. In the cases of Runner A, the angles of attack are about 5 deg. at near Q_{11}=1.04 m, m^3/s giving the maximum hydraulic efficiency. On the contrary, the angle to the rear blade of Runner B are obviously larger than the angle to the front blade at the lower discharge than Q_{11} = 0.72 m, m^3/s. That may be caused from the effect of the reverse flow occurring on the hub wall as follows.

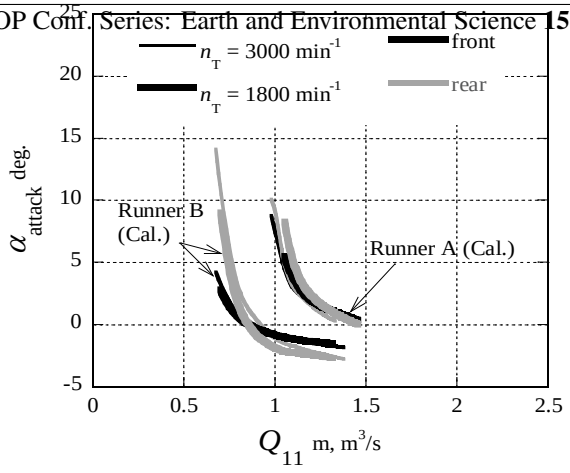

Figure 8. Angle of attack distributions at the root-mean square radius

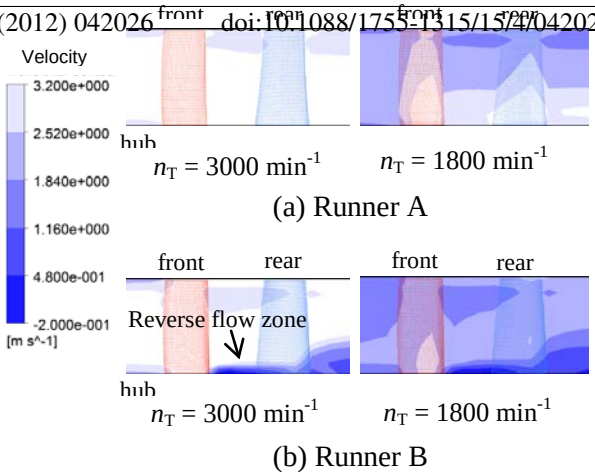

Figure 9. Velocity distributions on the meridian plane

To know the mechanism of the reverse flow occurring, the velocity vectors around the rear runner blades were simulated on the cylindrical plane in close to the hub wall (see figure 10). The flow attacks smoothly to the leading edge (L.E.) of the blade in Runner A, but the flow brings the local separation at the concave surface in Runner B due to the unacceptable camber for the turbine mode.

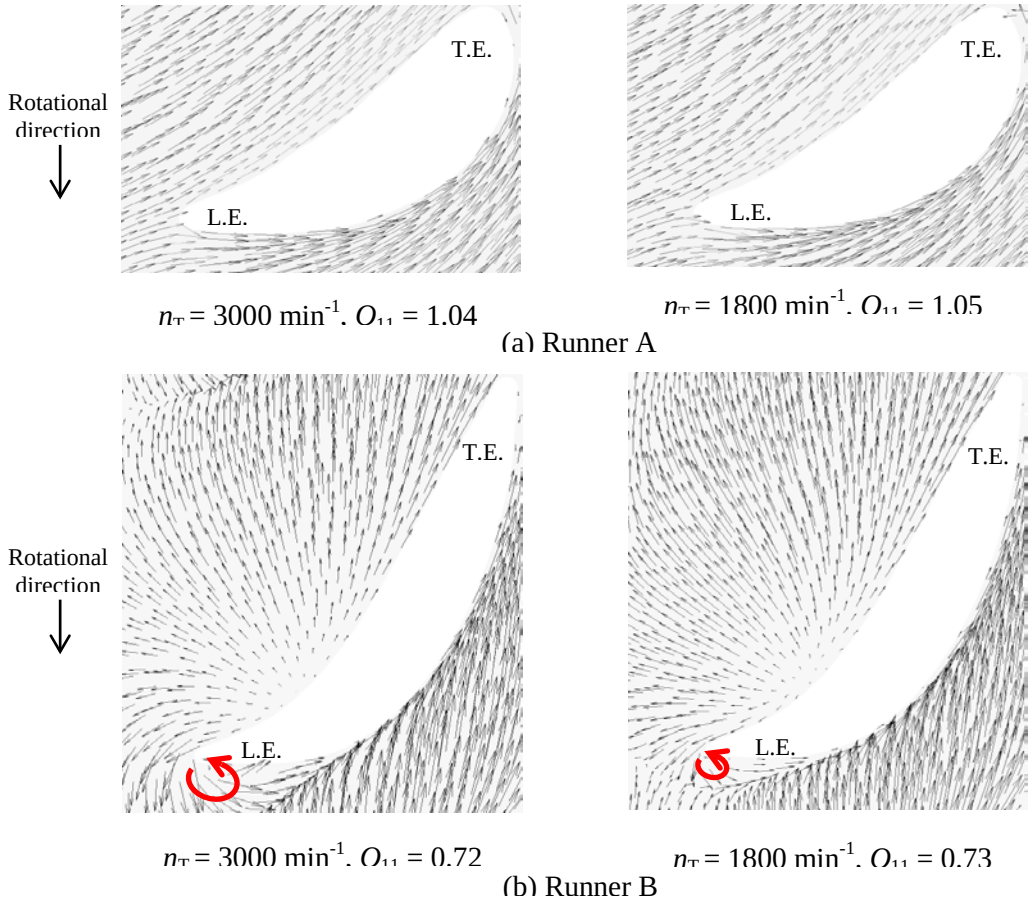

Figure 10. Velocity vectors on the cylindrical plane near hub wall (Y = 0.01)

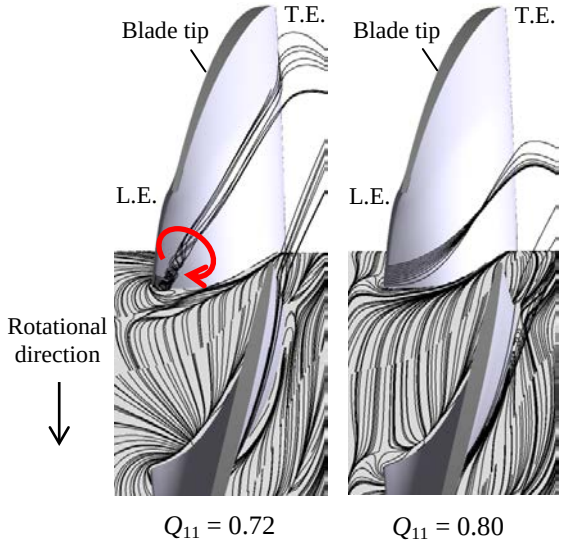

Figure 11. 3-D streamline originated at leading edge and limiting streamline on hub wall in the rear runner (Runner B, n_T = 3000 min^{-1})

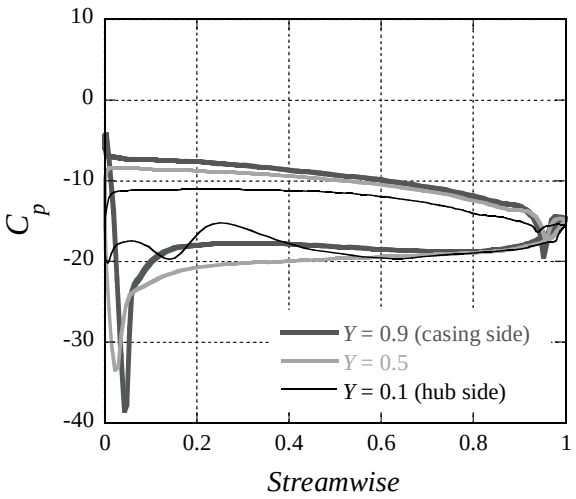

Figure 12. Blade loading distributions in the rear runner (Runner B, n_T = 3000 min^{-1}, Q_{11} = 0.72)

Figure 11 shows the 3-D streamline originated at the leading edge of the blade root and the limiting streamline on the hub wall in the rear runner. The flow through Runner B runs along the blade surface at Q_{11} = 0.80, but the flow forms the vortex in close to the leading edge at Q_{11} = 0.72. It is noticed that this clockwise vortex induced the secondary flow from the pressure side to the upstream of the neighbouring blade leading edge along the hub wall. Therefore, the abnormal flow makes the blade load higher with the increaser of the radius, as shown in figure 12 [$C_p = 2(p - p_0)/\rho/V_m^2$, p_0 and V_m: the static pressure and the meridian velocity at the section M0 in figure 1]. In addition, it can be reconfirmed that the runner blade with the sharp leading edge corresponding to the trailing edge in the pumping mode, such as Runner B, may be suitable for the lower discharge and the higher head, namely the low specific speed.

6. Conclusions

The counter-rotating type axial flow pump unit was provided for the turbine mode, and the following concluding remarks were obtained.

The maximum hydraulic efficiency in the turbine mode comes close to one of the counter-rotating type hydroelectric unit designed exclusively for the turbine mode.

The flow direction is axial at not only the inlet but also the outlet, regardless of the pumping/turbine mode and/or the blade profiles.

The runner with the sharp leading edge corresponding to the trailing edge in the pumping mode may be suitable for the lower discharge and the higher head, namely the low specific speed.

Acknowledgments

Some parts of this research were co-sponsored by Japan Society for the Promotion of Science KAKENHI 23860035.

References

[1] Kanemoto T, Kimura S, Ohba S and Satoh M 2000 Smart control of axial flow pump performances by means of counter-rotating type (1st report, counter-rotating type and performances) *JSME Series* B **66**(651) pp 2927-33 (in Japanese) & Kanemoto T and Oba S

2002 Proposition of unique pumping system with counter-rotating mechanism *Proc. 9th ISORMAC* FD-ABS-031

[2] Oba S, Kanemoto T and Fujimura M 2007 Rotational speed characteristics of counterrotating axial flow pump *Proc. 9th Asian Int. Conf. on Fluid Machinery* AICFM9-234 pp 1-6 & Kanemoto T, Komaki K, Katayama M and Fujimura M 2011 Counter-rotating type pumping unit (impeller speeds in smart control) *Int. J. of Fluid Machinery and Systems* **4**(3) pp 334-340

[3] Kanemoto T, Tanaka D, Kashiwabara T, Uno M and Nemoto M 2001 Tidal current power generation system suitable for boarding on a floating buoy *Int. J. of Offshore and Polar Engineering* **11**(1) pp 77-79

[4] Kanemoto T, Tominaga K, Tanaka D, Sato T, Kashiwabara T and Uno M 2002 Development of counter-rotating type machine for hydroelectric power generation (2nd report, hydraulic performance and potential interference of counter-rotating runners) *JSME Series* B **68**(676) pp 3416-3423 (in Japanese)

[5] Tanaka D and Kanemoto T 2006 Experimental study on design materials for solidity of counter-rotating runners *Proc. 23th IAHR Symp.* F147

[6] Nielsen T K, Royrvik J, Ramdai J and Dahlhaug O G 2006 Propeller turbine with two contra-rotating impellers and built in generator *Proc. 23th IAHR Symp.* F146

[7] Joseph L H, et al. 1951 Systematic two-dimensional cascade tests of NACA 65-series compressor blades at low speed *NACA Tech. Note* 3916

[8] Oba S and Kanemoto T 2004 Performance comparison by design change of counter-rotating impeller *Proc. 22nd IAHR Symp.* **B** pp B09-1 doc-1(9)-B09-1 doc-9(9)

[9] Tanaka D and Kanemoto T 2006 Development of counter-rotational type machine for hydroelectric power generation (3rd report, design materials for solidity of axial flow runners) *JSME Series* B **72**(715) pp 686-692 (in Japanese)

[10] Itou S, Fujimura M, Nonoue S and Kanemoto T 2009 Counter-rotating type pump unit (rotational behaviors) *Proc. 10th Asian Int. Conf. on Fluid Machinery* Paper ID: 159

[11] Kanemoto T and Suzuki T 2010 Counter-rotating type hydroelectric unit suitable for tidal power station *Proc. 25th IAHR Symp. on Hydraulic Machinery and Systems* Paper No. 11A 5 1755-1315/12/1/012111